Polymer Brush Electrets

*Xinlei Ma, Zhuang Xie, Zhilu Liu, Xuqing Liu, Tingbing Cao, and Zijian Zheng**

Dedicated to the memory of co-author Tingbing Cao, deceased March, 2012

The charge storage properties of polymer brushes are reported for the first time. Poly(methyl methacrylate) (PMMA) brushes are explored as electrets to store electrostatic charges. Micrometer- and nanometer-scale patterns of electrostatic charges are successfully fabricated on planar and non-planar PMMA brush films by means of conductive microcontact printing and atomic force microscope lithography, where the charge storage density and stability are studied in detail with Kelvin force microscopy. Importantly, because PMMA brushes are chemically tethered on the substrate, their charge storage properties can be studied in various organic solvents, in which their bulk counterparts will be dissolved. It is found that patterned charges on PMMA brushes are stable enough in organic media, such as hexane and toluene, for guiding the assembly of Au nanoparticles in organic media and the dewetting of polymer thin films with solvent annealing. The electrets properties shall add a new dimension of functionality, apart from the conventional chemical and physical properties, to polymer brushes for a wide range of applications in materials science, nanotechnology, and electronic devices.

1. Introduction

The tailoring of surface properties with polymer brushes has been an increasingly active field for a wide variety of researches and applications ranging from material science, nanotechnology, electronics to biological and medical systems.[1–3] With one end of the polymer chain tethering to a substrate, polymer brushes exhibit excellent environment robustness and well-organized chain conformation, which endow superior control over surface structures and functionalities such as film morphology, grafting density, chemical composition, and many other surface properties different from bulk counterparts.[4] By using lithographic tools and surface-initiated polymerization strategies, micro and nanoscale complex surface architectures can be readily constructed with polymer brushes on a wide range of surfaces.[5,6] As such, polymer brushes have been considered as "soft" building blocks for micro/nanofabrication and controlled assembly of small objects,[7–11] sensors and actuators,[12–18] electronics,[19–21] anti-fouling coatings and biocompatible surfaces.[22–25] Among these literatures, the realization of functionality is mostly based on the rational design of the chemical functional groups of polymer brushes. For instance, polymer brushes with ionic side groups were extensively exploited to entrap counter ions or nanoparticles (NPs).[26,27] Patterned polymer brushes with hydrophobic and hydrophilic domains were utilized to direct self-assembly and phase separation of block copolymers.[28]

Apart from chemical functionality, another simple and effective way to realize functional surfaces and tune interfacial properties is to introduce the electrostatic charge. Materials that trap net electrostatic charges, namely electrets, have shown fruitful applications in electronic, mechanic and biological systems. For example, patterns of electrostatic charges are widely used in conventional xerography, as well as templates to induce the self-assembly of micro/nanoparticles,[29–35] macromolecules[36–38] and other building blocks[39] with resolution as small as sub-100 nm. Electrostatic charges can also initiate redox reactions in situ[40–42] and control the behavior of thin film electronic devices.[43–45] To date, although many materials such as SiO_2 and casted polymer thin films have been demonstrated as effective electrets, the fundamental question of whether polymer brushes can trap electrostatic charges remains unknown. In principle, neutral polymer brushes should be electrets because the dielectric constant of polymer brushes is similar to that of the bulk polymer thin film. Considering that polymer brushes can be readily grown and structured on many substrates, especially those that are non-planar, we believe that the introduction of electrostatic charge into polymer brushes shall add a new dimension for surface functionalization apart from alternating the chemical structure of the brushes.

X. L. Ma, Prof. T. B. Cao
Department of Chemistry
Renmin University of China
Beijing 100872, China
X. L. Ma, Z. Xie, Dr. Z. L. Liu,
X. Q. Liu, Prof. Z. J. Zheng
Nanotechnology Center
Institute of Textiles and Clothing
The Hong Kong Polytechnic University
Hung Hom, Kowloon, Hong Kong SAR, China
E-mail: tczzheng@polyu.edu.hk
Z. Xie, Dr. Z. L. Liu, Prof. Z. J. Zheng
Advanced Research Centre for Fashion and Textiles
The Hong Kong Polytechnic University Shenzhen Research Institute
Shenzhen 518000, China

DOI: 10.1002/adfm.201203181

In this paper, we report the first study on the trapping ability of electrostatic charges in polymer brushes, and the application of charged polymer brushes as effective templates for guiding the self-assembly of Au nanoparticles (Au NPs) and dewetting of polymer thin films. Poly(methyl methacrylate) (PMMA) brushes are for the first time demonstrated as electrets, which can store quasi-permanent electrostatic charges. Positive and negative electrostatic charges are patterned on PMMA brushes by using the conductive atomic force microscope (AFM) tip or Au-coated polydimethylsiloxane (PDMS) stamp as working electrode. Compared with bulk polymer thin films, polymer brush electrets exhibit several advantages. First, it is easy to prepare densely packed, pinhole-free polymer brush film with controlled thickness. Second, polymer brushes are versatile for uniform coating on various surfaces including topographic and curved ones. More importantly, because polymer brushes are tethered on the substrate even in their good solvent, it allows the study of electrostatic charge stability in various organic solvents, which further enables the directed assembly of Au NPs and dewetting of polymers in toluene using PMMA brush electrets as template. It should be noted that in previous studies, such experiments cannot be achieved on templates using bulk polymer thin films as non-tethered polymer chains are readily washed away by organic solvents.

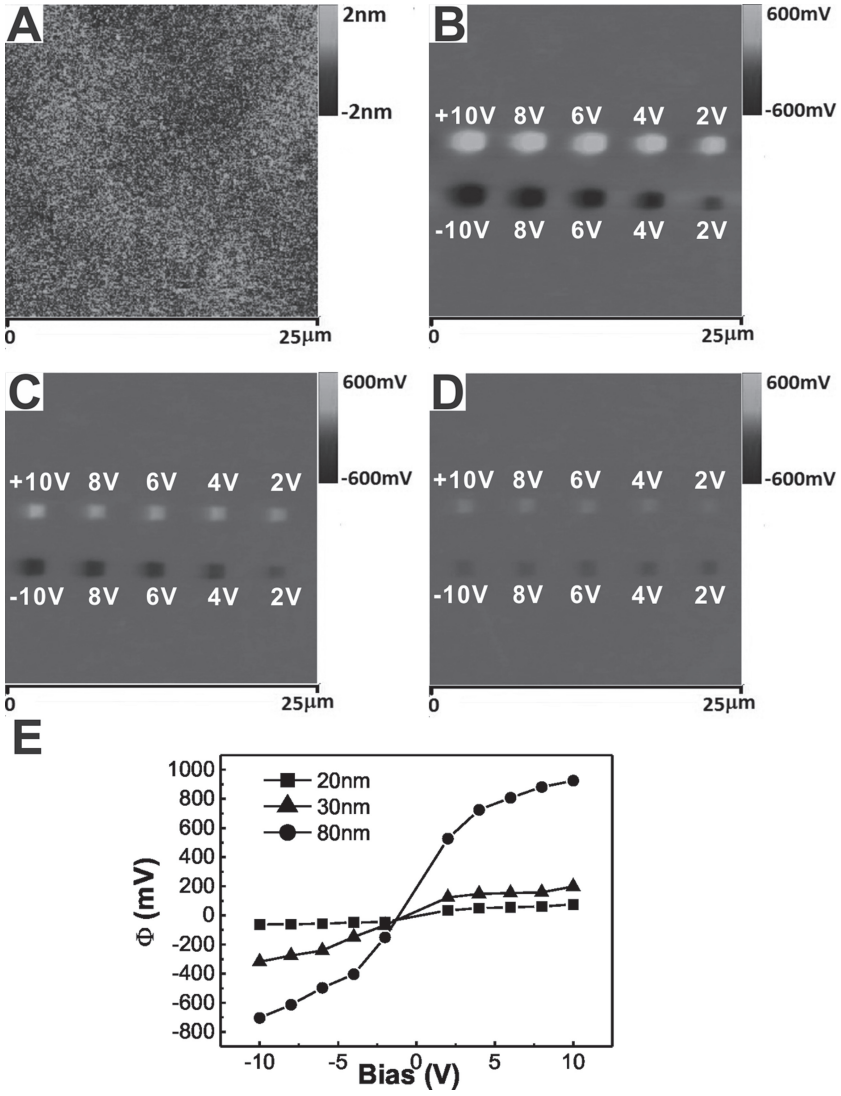

Figure 1. The dependence of surface potential on brush thickness and applied DC voltage. A) AFM topography of PMMA brushes after charge patterning. B–D) KFM images of trapped charges patterned in PMMA brushes of different thickness (B: 80 nm, C: 30 nm, D: 20 nm). The square patterns of charges were written at 4 Hz scanning, under ±10 V to ±2 V from left to right. E) Plot of the surface potential of charge patterns at different brush thicknesses as a function of the applied bias.

2. Results and Discussion

2.1. Charge Patterning on PMMA Brushes

PMMA brushes were prepared on Au substrates by surface-initiated atom transfer radical polymerization (SI-ATRP) following previous procedures.[46] Briefly, an Au-coated n-doped Si substrate was modified with a self-assembled monolayer (SAM) of thiol initiator molecules, ω-mercaptoundecyl bromoisobutyrate (MUDBr). The substrate was then placed into an aqueous solution containing $CuBr/CuBr_2$/2,2-dipyridyl to grow PMMA brushes via SI-ATRP (see the Experimental Section for details). The thickness of the PMMA brushes was controlled by varying polymerization time. The prepared PMMA brushes were highly uniform and pinhole-free, with a surface roughness (R_q) of ~1 nm (**Figure 1**A).

PMMA brushes were then locally charged to fabricate charge patterns using either a conductive AFM tip or a Au-coated PDMS stamp as working electrode at a humidity of 50–60% in air, as shown in **Scheme 1**. The working electrode was brought into contact with the PMMA brushes and an external voltage was applied between the working electrode and the Au substrate. Nanodots and nanolines of electrostatic charges were fabricated with conductive AFM with a DC voltage (ca. –10 to +10 V) applied on the tip. The conductive AFM tip is a high-resolution and flexible tool to inject charges into the electrets for studying the charge storage performance, with precise control of the position, size, shape and applying voltage. On the other hand, the Au-coated PDMS stamp was used to parallelly print microlines and dots of charges on polymer brushes over large areas, which is suitable to study the charge stability in air and organic solvents, and to fabricate templates for directed assembly of NPs and polymers. The as-made charge patterns were characterized by Kelvin force microscopy (KFM).

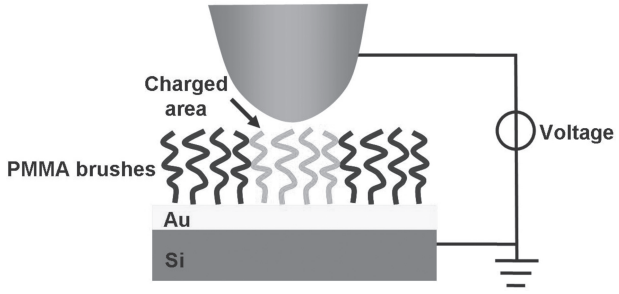

Scheme 1. Schematic illustration of the charge fabrication process on PMMA brush electrets using conductive atomic force microscope (AFM) tip or Au-coated polydimethylsiloxane (PDMS) stamp. An external voltage is applied either on the conductive AFM cantilever in contact mode or on the Au-coated PDMS stamp which is brought into conformal contact with the PMMA brush layer.

2.2. Charge Storage Properties of Polymer Brushes

As a proof-of-concept experiment to show that polymer brushes can be used as electrets, a series of 1 μm × 1 μm squares of electrostatic charges were fabricated on PMMA brushes (thickness = 80, 30, or 20 nm) by scanning the conductive AFM tip at 4 Hz with different applied bias ranging from ±10 V to ±2 V. Indeed, both positive and negative surface potential shifts were measured by KFM (Figure 1B–D), while no obvious topography change of the polymer brush surface was observed (Figure 1A). This phenomenon is a typical characteristic of electrets, which indicates that the positive and negative charges can be trapped in the PMMA brushes due to charge injection. Under the same applied voltage, the amount of charge storage showed distinct brush thickness dependence, i.e., thicker brush exhibited higher capability in charge storage. For example, on the 80 nm thick brushes, the surface potential shifts reached ~900 mV and ~700 mV upon positive and negative charging at 10 V respectively, while the surface potential shifts for both negative and positive charges did not exceed 80 mV on the 20 nm thick brushes. We also found that amount of charge storage increased as the writing bias increased. This is especially obvious in thicker brushes. On 80 nm thick PMMA brushes, the surface potential shift increased from ~530 mV to ~930 mV when the applied bias increased from 2 V to 10 V. It is noted that the high amount of charging was accompanied with the lateral spreading of electrostatic charges. Therefore, as a balance between patterning resolution and charging amount, the rest of the experiments were taken out on the PMMA brush film with a thickness of ~40 nm and the applied bias of 8 V. The charge storage behavior of PMMA brushes was similar to the previous reports on the bulk polymer thin film electrets,[47,48] where pulse voltage was used for AFM charge writing: the film thickness determined the maximum surface potential that could be generated, and the amount of the trapped charges including both the surface potential and the size of charge patterns increased linearly with the increasing pulse voltage.

We then studied the charge diffusion during the charge injection process at high resolution. The conductive AFM tip was made into contact with the PMMA brushes (43 nm thick) from 5 ms to 90 s to generate nanodots of electrostatic charges at a constant bias of ±8 V (**Figure 2**A). The smallest dot can be obtained at the dwell time of 5 ms for both positive and negative charges, with the full width half maximum (FWHM) of ~ 150 nm. Importantly, the surface potential and the size of the written dots both increased with longer dwell time due to the charge injection and the lateral spreading during the writing process (Figure 2B,C). It was reported that the surface potential (Φ) of the charged areas could be approximately considered as a linear function of the trapped surface charge density.[32,49] Therefore, we can estimate the amount of surface charges (Q) in each written dot by equation:

$$Q = \frac{\varepsilon \times \Phi \times S}{d \times e}$$

where ε is the permittivity of PMMA (2.6×10^{-11} C/(Vm)), d is the thickness of the PMMA brushes, S is the dot area, and e is the elementary charge (1.6×10^{-19} C). According to ref. [29], for a double layer separated by a distinct distance d, the charge density can be calculated with $\varepsilon\Delta V/d$. Therefore, the surface charge densities that can be achieved with the PMMA brushes are 3.4×10^{-4} C/m^2 or 2.1×10^3 elementary charges/μm^2 for positive charges (Φ ~1 V, d = 80 nm), and 2.7×10^{-4} C/m^2 or 1.7×10^3 elementary charges/μm^2 for negative charges (Φ ~0.8 V, d = 80 nm). Figure D shows the calculated Q as a function of dwell time, where Q is fitted to be proportional to $1\text{-}e^{-t/\tau}$, indicating that the charging process on the brush film is similar to that of a conventional capacitor. Apart from nanodots, we also patterned nanolines of electrostatic charges by scanning the conductive AFM tip on the PMMA brushes with different tip speed ranging from 0.05 μm/s to 40 μm/s. Again, we found similar charge diffusion results compared with nanodots (Figure 2E–G), where slower tip speed lead to the higher surface potential and larger line width. The amount of electrostatic charges in each line can be fitted to be proportional to $1\text{-}e^{-1/v\tau}$, where v is the tip speed.

2.3. Charge Stabilities

The stability of the trapped charges in PMMA brush electrets was first studied by measuring the surface potential of the charge patterns after storing in ambient conditions for a certain period of time. The relative humidity of the environment was ~65% during the whole experiment. Charge patterns with surface potentials of ±700 mV were fabricated. As indicated from **Figure 3**A, the surface potential decayed to half of its value per day and reached a noise level of the KFM after storing for 6 days. It was reported that, at room temperature, the surface charges in the electrets decayed by both external neutralization and internal diffusion. On one hand, the decay was attributed to the adsorption of counter ions from the surrounding medium, which neutralized the surface charges. Meanwhile, the small electrical conductivity of electrets and the diffusion of charge carriers could also cause the loss of charges.[47] Considering that the sample was stored at a relatively high humidity, we believe that the decay of charges can be mainly attributed to the external neutralization mechanism.

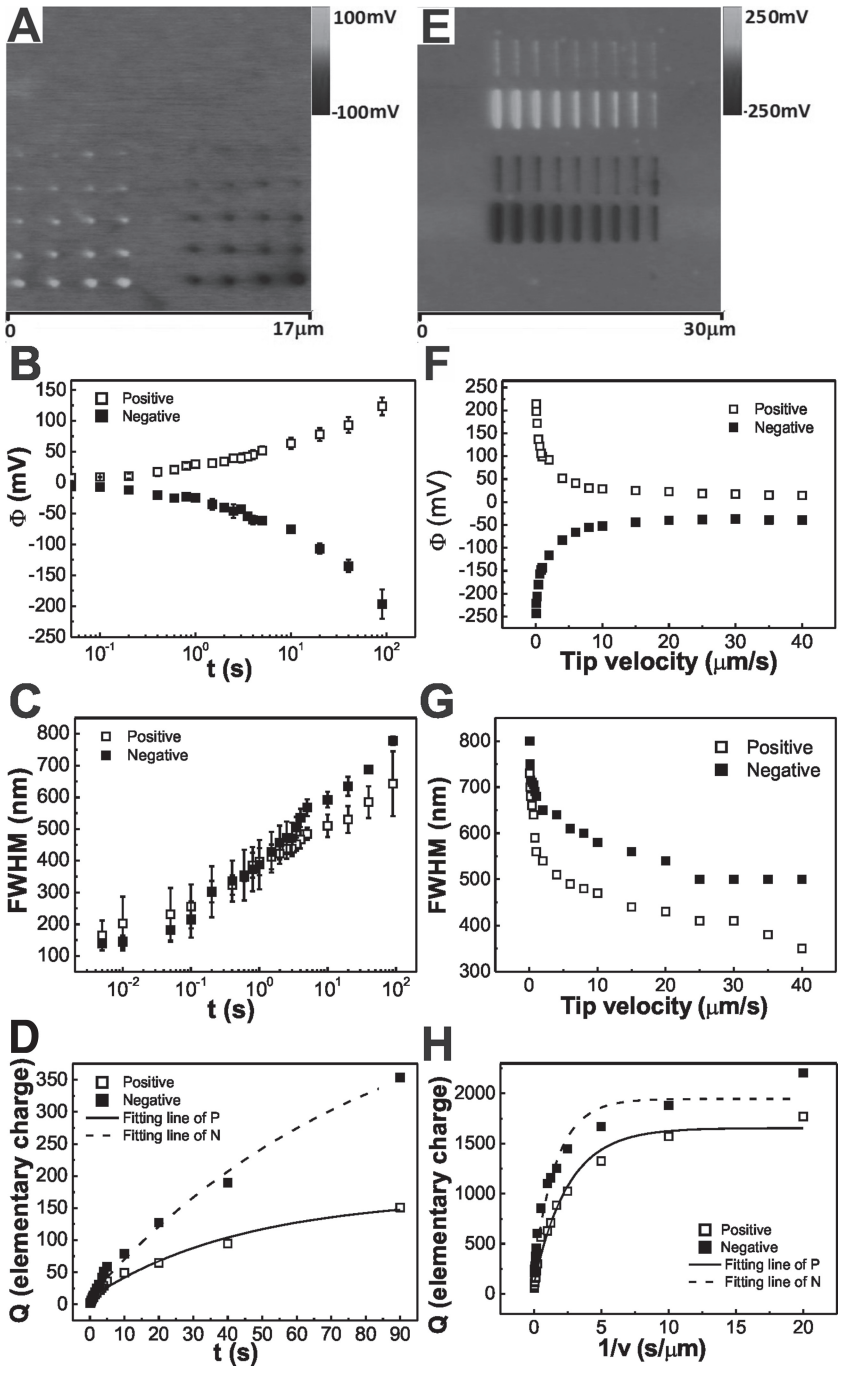

Figure 2. A) KFM image of trapped charges patterned with different dwell time. B–D) Plots of surface potential, FWHM, and charge amount Q as a function of the dwell time t. Q is fitted as $Q \propto (1\text{-}e^{-t/\tau})$. (E) KFM image of trapped charges patterned with different tip speed. F–G) Plots of surface potential and FWHM as a function of the tip speed v. H) Plot of charge amount Q with $1/v$. Q is fitted as $Q \propto (1\text{-}e^{-1/v\tau})$

of the heater was fixed at 60 °C and the sample was characterized continuously for ~250 min. Indeed, the charge decay occured soon after heating and the surface potential dropped to ~10% after 250 min as shown in Figure 3B. Since the heating temperature was below the T_g of PMMA, the charge decay can be ascribed to the local rotational relaxation of the chemical groups on the polymer chains.

Owing to solvent resistance of polymer brushes, the stability of trapped charges in different organic solvents can be studied without considering the dissolution of electrets materials. It should be noted that these kinds of measurements in organic solvent were only applicable to non-solvents for bulk polymer thin films in the previous studies. In our case, we chose good solvents (toluene, acetone, chloroform, ethyl acetate), a poor solvent (N, N-dimethylformamide), and a non-solvent (hexane) for PMMA respectively, to study solvent stability of trapped charges. Samples were charged with Au-coated PDMS stamp. After the charging process, samples were immersed in different solvents for 5 s, and then blow-dried with compressed air for KFM characterization (Figure 3C). After immersing in hexane, the residual surface potential on PMMA brush electrets remained at 83% of that after charge patterning. On the contrary, after immersing in toluene, the surface potential decreased dramatically to ~23% when compared with the original charges. And more than 95% of charges decayed after 5 s of immersing in polar solvents, resulting in surface potential close to the noise level (<10 mV). This difference may be attributed to the chain movement and polarity of the solvents. PMMA brushes swell in good and poor solvents of PMMA but cannot be dissolved to form free polymer chains, thus the trapped charges on PMMA brushes will not disappear completely when immersed in organic solvents for short times. However, there may be a major loss in charges due to the chain swelling. In addition, polar solvents were polarized by the electric field generated by the charged electrets and neutralize the charges. As a consequence, polar solvents had a greater charge neutralization effect in decreasing surface potential. Note that impurities in the organic solvents may also induce charge loss.[47] In hexane, a nonpolar and non-solvent for PMMA, the effects on both charge dissipation and brush swelling are small and the charge stability was much improved.

Since heat will also neutralize the charges or release the dipoles through a process called thermally stimulated discharge or depolarization (TSD), the charge stability during heating was also investigated by heating the charge-patterned PMMA brush electrets and measuring the surface potential with KFM in real-time. To obtain stable KFM signals, the temperature

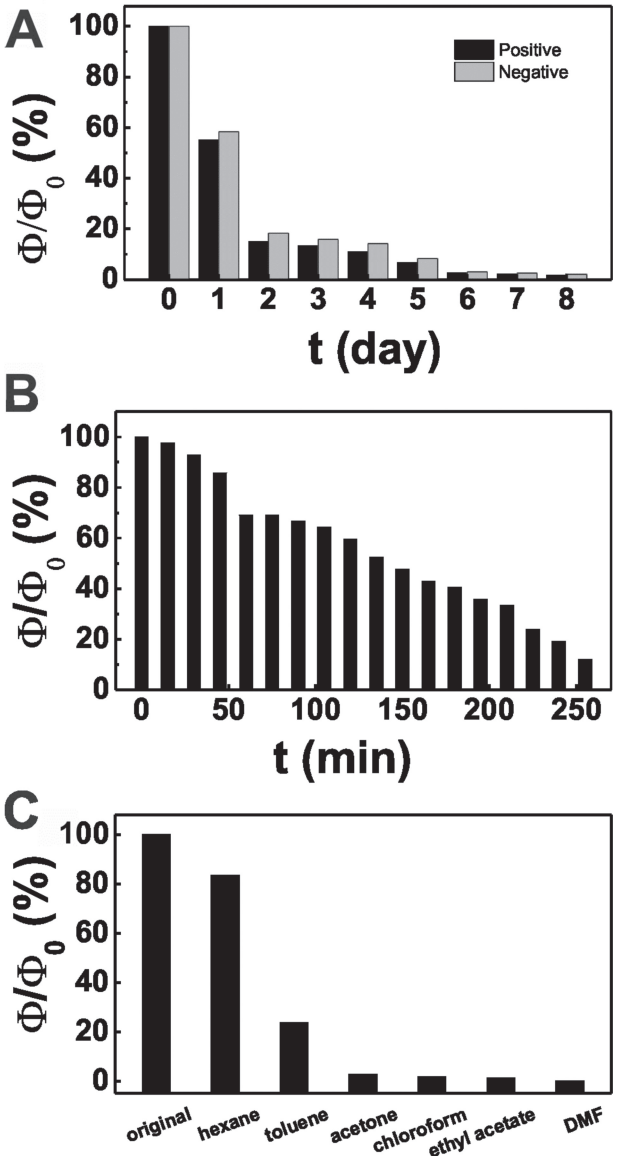

Figure 3. Stability of the charges. A) The decay of charges in PMMA brushes after storing in ambient conditions and room temperature for 8 days. B) The stability of the trapped charges in PMMA brushes at 60 °C in air. C) The stability of trapped charges in different solvents.

2.4. Comparison Between PMMA Brushes and Bulk PMMA Thin Films as Electrets

From our experimental results, PMMA brushes were found to exhibit charge storage properties similar to those of PMMA thin films, in terms of surface potential value, the patterning resolution of charge patterns under similar charging processes, and charge stability at the room temperature and 60 °C in air (Supporting Information Figure S1). These results indicate that the amount of trapped charges was mainly determined by the polymer used and not the configuration arrangement, i.e., brush or bulk, of polymer chains.

On the other hand, polymer brushes outweigh their bulk counterparts on charge stability in organic solvents. Because polymer brushes are chemically tethered on the substrate, trapped charges generated in air can still survive in various organic solvents, while the stability is influenced by the chain swelling of polymer brushes and the polarity of the solvent. On the contrary, trapped charges in the bulk polymer thin films can only exist in non-solvents of the polymer (e.g., ethanol and DI-water for PMMA).

In addition, polymer brushes with uniform thickness can be readily grown on non-planar surfaces through the SI-ATRP process, so that polymer brush electrets are also compatible with applications requiring surface topographies. As proof-of-concept, we demonstrate here the charge patterning of PMMA brushes on a topographic surface. 40-nm-thick PMMA brushes were grown on a Au-coated Si substrate, of which arrays of square microwells (40-μm edge length, 400-nm depth) have been fabricated by a typical microfabrication method (see the Experimental Section for details). After polymerization, the depth of the PMMA brush coated microwells remained at 400 nm, indicating that the whole topographic substrate was coated evenly with PMMA brushes (Supporting Information Figure S4B). Subsequently, conductive AFM was used to pattern charges the PMMA brushes both on the bottom and the bank of the microwells at ±10 V (**Figure 4**, indicated by the dash square). Very importantly, the amounts of the trapped charges at the two areas were found to be identical, which can be attributed to the uniform growth of the PMMA brushes. In contrast, PMMA thin films fabricated by spin-coating bulk PMMA on the microwells cannot form uniform coating (Figure S4C) so that the amount of trapped charges are not uniform and are difficult to control over the whole topographic surface.

2.5. Guided Assembly on Charge-Patterned PMMA Brush Templates

Because PMMA brushes show much superior charge stability in solvents to that of bulk PMMA thin films, the charge patterns on polymer brush electrets are promising templates to direct the assembly of nanomaterials in organic solvents. As proof-of-concept, we demonstrate here two examples using charge-patterned PMMA brushes as template for guiding the assembly of NPs and the dewetting of bulk polymer thin films in the media of toluene.

In the first example, negative charge-patterned PMMA brushes were immersed in the toluene solution of positively charged Au NPs for 5 s, removed from the solution, and dipped in MilliQ water to rinse away the loosely adsorbed particles. It is found that most of the Au NPs adsorbed to negatively charged areas due to electrostatic interaction and a few Au NPs adsorbed to uncharged areas by physisorption. Since the electric field gradient is stronger on the edges of the line patterns, denser clusters of nanoparticles were found there. Note that the conventional xerography on PMMA thin films can only be performed in non-solvents of PMMA, such as ethanol.

In the second example, we show that charge-patterned PMMA brushes can be used as templates for guiding the self-organization of polymer thin films. In the previous

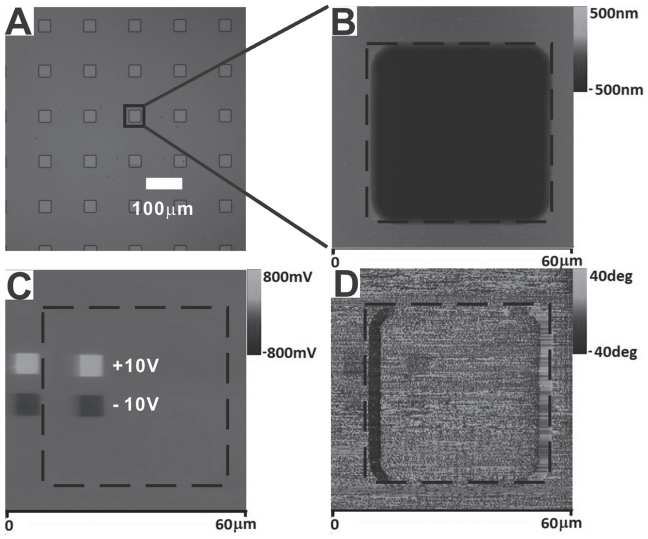

Figure 4. Charge patterning on non-planar surfaces. A) Optical microscope image of PMMA brushes grown on Au-coated Si substrate patterned with square microwells (40-μm side length, 400-nm depth). B–D) Zoom-in AFM, KFM, and phase images of the charged area at the boundary of a microwell highlighted in (A).

3. Conclusions

For the first time, we have demonstrated that polymer brushes are a new kind of electrets material that can be effectively and rationally charged, both positively and negatively, by means of conductive microcontact printing and AFM lithography. The charge storage performance of PMMA brush electrets is similar to that of bulk PMMA thin films in terms of charge amount, patterning resolution, and air stability at room temperature and 60 °C. Importantly, because PMMA brushes are grown by SI-ATRP, it allows the fabrication of uniform charge patterns on non-planar surfaces. This advantage can potentially lead to new applications such as the formation of spatially confined electric field distributions or hierarchical structures. More importantly, we have reported the first study on charge stability of PMMA in organic solvents, due to the fact that surface-tethered PMMA brushes are stable even in their good solvents. The trapped charges in PMMA brushes are found to be durable in organic solvents such as hexane and toluene. The xerography of Au NPs and surface dewetting of polymer thin films are demonstrated using PMMA brush electrets as templates in toluene. In contrast, there experiments cannot be achieved with conventional bulk PMMA electrets, which dissolve in toluene.

reports, the self-organization of polymers on charge patterns was only demonstrated on inorganic electrets because the process required polymer film casting with organic solvents and subsequent annealing in their vapors.[37,38] In our case, polystyrene (PS) in toluene (0.5 wt%) was spin-coated on charge-patterned PMMA brushes (**Figure 5**D,G) to form a 20-nm-thick PS film. The charge patterns were 2 μm × 12 μm line arrays and 3 μm × 8 μm dot arrays. The sample was then annealed in a toluene vapor for 48 h and blow-dried with compressed air. It is observed that surface dewetting of the PS thin film occurred and dewetting patterns followed the underlying charge patterns very well (Figure 5E,H). The samples were further characterized by optical microscope so that the periodicity of the polymer structures can be confirmed by performing a fast Fourier transform (FFT) (insets of Figure 5F,I). Indeed, the high-intensity spot arrays in FFT images reflect that the periodicity of the dewetted structures equals to that of center-to-center distance of the corresponding underlying charge patterns. The main driving force for the assembly is the electric field caused by trapped charges and the destabilization forces between the substrate (PMMA brush) and the PS. As a control experiment, PS was made to dewet on uncharged PMMA brushes following the same procedures and no periodic dewetting pattern was observed.

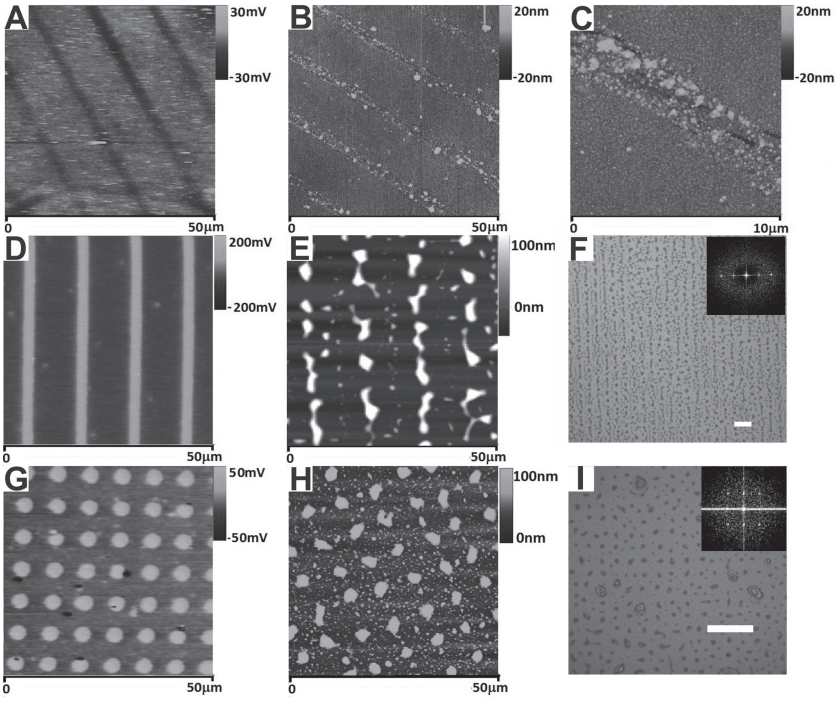

Figure 5. Guided assembly on charge patterns fabricated on PMMA brush electrets. A) KFM image of negative charge patterns. B,C) AFM images of the assembled positively charged Au NPs using charge patterns shown in (A) as template. D) KFM image of the line patterns of positive charges. E) AFM topography and F) optical microscope image of the dewetted PS film using D) charge patterns as the template. G) KFM image of positive charge patterns. H) AFM topography and I) optical microscope image of the dewetted PS film using G) charge patterns as the template. FFT images of the optical images are inserted in (F) and (I), respectively, showing that the periodicity of the dewetted PS patterns follows that of the charge template. The scale bars are 20 μm.

4. Experimental Section

The initiator ω-mercaptoundecyl bromoisobutyrate (MUDBr) was synthesized according to the literature.[46] Other chemical reagents were purchased from Aldrich and used as received. All the AFM and KFM images were recorded using a Bruker NanoScope 8 and the SEM images were recorded with a JEOL 6490 microscope. The charge writing was taken out using XE-100 (Park Systems). Fast Fourier transforms (FFT) were performed using ImageJ software.

Preparation of PMMA Brushes: The Au-coated n-doped Si wafer (5 nm Cr, 50 nm Au) was immersed into a 1 mM MUDBr ethanol solution overnight and rinsed with fresh ethanol. PMMA brushes were then grown on the substrate through surface-initiated atom transfer radical polymerization (SI-ATRP) in aqueous media:[46] the MUDBr-coated Au substrate was placed in Schlenk tubes under a N_2 atmosphere at ≈35–40 °C, followed by adding the degassed monomer solution. Typically, the monomer solution used to prepare PMMA brushes is composed of 5 g MMA, 4 mL of methanol, 1 mL of DI water, Cu(I)Br (0.071 g), 2,2-dipyridyl (0.156 g). The polymerization time was varied from 1 to 8 h to control thickness. After reaction, the resultant substrates were rinsed extensively with methanol, DI water and toluene, and then dried under a stream of N_2.

Fabrication of Non-Planar Substrates: A Si wafer with a 500 nm silica layer was spincoated with a positive photoresist HPR-507. Patterns of 40 μm × 40 μm square wells were fabricated on the photoresist by photolithography. After being exposed to oxygen plasma for 1 min, the exposed silica layer was etched with a buffered solution of HF to obtain 40 μm × 40 μm wells with a depth of 400 nm, and the photoresist was rinsed away with acetone. Finally, the patterned Si substrate was coated with 5 nm Cr and 100 nm Au by thermal evaporation.

Charge Patterning: XE-100 (Park Systems) was used for conductive AFM lithography with conductive AFM tips (SCM-PIT, Veeco) in contact mode. A positive or negative DC bias was applied on the tip, and the tip was approached to the substrate for charge patterning. Alternatively, an Au-coated PDMS stamp was also used for charge patterning. A bias of ±10 kV/cm was applied between the stamp and the substrate using a Keithley 2400 source-meter for 20 s.

Synthesis and Self-Assembly of Au NPs: The synthesis of thiol-terminated Au NPs (~5 nm in diameter) in toluene follows a procedure in the literature.[50] Briefly, 1 mL $HAuCl_4$ (1 wt% in water) was added to 90 mL DI-water at room temperature. The mixture was stirred for 1 min, and 2 mL sodium citrate aqueous solution (38.8 mM) was added. After stirring for 1 min, 1 mL $NaBH_4$ aqueous solution (0.075 wt% in 38.8 mM sodium citrate) was added, and this mixture was further stirred for 5 min to yield an Au colloidal solution. Subsequently, 10 mL dodecanethiol in toluene (50 mM) was mixed with 5 mL as-made Au colloidal solution, and 5 mL phase transfer agent tetraoctylammonium bromide (TOAB) aqueous solution (50 mM) was added. Under stirring, the Au colloids were transferred into the organic phase and formed dodecanethiol-terminated Au NPs.[33] The patterned charged PMMA brushes were immersed in the toluene solution of dodecanethiol-terminated Au NPs for 5 s, and then removed from the solution and dipped in DI water to resin the loosely attached particles.

Surface Dewetting of Polymer Thin Films: 0.5 wt% polystyrene (PS, Mw = 96 kg mol^{-1}) in toluene was spincoated onto the charge-patterned PMMA brushes at 4000 rpm for 20 s. The substrate was then annealed in a toluene vapor environment for 48 h.

Supporting Information

Supporting Information is available from the Wiley Online Library or from the author.

Acknowledgements

Z.J.Z. acknowledges General Research Fund of Hong Kong (Project PolyU 5041/11P), The Hong Kong Polytechnic University (Project A-PK21), and The National Natural Science Foundation of China (Project 51273167) for financial support of this work. The authors acknowledge Prof. Hongwei Ma at Suzhou Institute of Nano-Tech and Nano-Bionics (SINANO), CAS, for providing the initiators, Prof. Qian Miao and Danqing Liu at The Chinese University of Hong Kong for thermal evaporation, Prof. Hongkai Wu and Yihua Zhao at Hong Kong University of Science and Technology for the help in photolithography, and Ms. Lily Chan for proof-reading the language. This article was amended after online publication. In the original version, the unit "μm" was erroneously printed as "mm" in several places and the affiliation section contained incorrect information.

Received: October 30, 2012
Revised: December 19, 2012
Published online: January 28, 2013

[1] R. Barbey, L. Lavanant, D. Paripovic, N. Schuwer, C. Sugnaux, S. Tugulu, H. A. Klok, *Chem. Rev.* **2009**, *109*, 5437.
[2] M. A. C. Stuart, W. T. S. Huck, J. Genzer, M. Muller, C. Ober, M. Stamm, G. B. Sukhorukov, I. Szleifer, V. V. Tsukruk, M. Urban, F. Winnik, S. Zauscher, I. Luzinov, S. Minko, *Nat. Mater.* **2010**, *9*, 101.
[3] O. Azzaroni, *J. Polym. Sci., Part A: Polym. Chem.* **2012**, *50*, 3225.
[4] S. V. Orski, K. H. Fries, S. K. Sontag, J. Locklin, *J. Mater. Chem.* **2011**, *21*, 14135.
[5] T. Chen, I. Amin, R. Jordan, *Chem. Soc. Rev.* **2012**, *41*, 3280.
[6] X. Zhou, X. Liu, Z. Xie, Z. Zheng, *Nanoscale* **2011**, *3*, 4929.
[7] U. Schmelmer, A. Paul, A. Kuller, M. Steenackers, A. Ulman, M. Grunze, A. Golzhauser, R. Jordan, *Small* **2007**, *3*, 459.
[8] M. Y. Paik, Y. Y. Xu, A. Rastogi, M. Tanaka, Y. Yi, C. K. Ober, *Nano Lett.* **2010**, *10*, 3873.
[9] X. C. Zhou, X. L. Wang, Y. D. Shen, Z. Xie, Z. J. Zheng, *Angew. Chem. Int. Ed.* **2011**, *50*, 6506.
[10] M. S. Onses, C. J. Thode, C. C. Liu, S. X. Ji, P. L. Cook, F. J. Himpsel, P. F. Nealey, *Adv. Funct. Mater.* **2011**, *21*, 3074.
[11] G. J. Dunderdale, J. R. Howse, J. P. A. Fairclough, *Langmuir* **2011**, *27*, 11801.
[12] P. Uhlmann, H. Merlitz, J. U. Sommer, M. Stamm, *Macromol. Rapid Commun.* **2009**, *30*, 732.
[13] T. Chen, R. Ferris, J. M. Zhang, R. Ducker, S. Zauscher, *Prog. Polym. Sci.* **2010**, *35*, 94.
[14] J. Bunsow, T. S. Kelby, W. T. S. Huck, *Acc. Chem. Res.* **2010**, *43*, 466.
[15] I. Tokareva, S. Minko, J. H. Fendler, E. Hutter, *J. Am. Chem. Soc.* **2004**, *126*, 15950.
[16] L. Ionov, S. Sapra, A. Synytska, A. L. Rogach, M. Stamm, S. Diez, *Adv. Mater.* **2006**, *18*, 1453.
[17] S. Gupta, M. Agrawal, M. Conrad, N. A. Hutter, P. Olk, F. Simon, L. M. Eng, M. Stamm, R. Jordan, *Adv. Funct. Mater.* **2010**, *20*, 1756.
[18] T. Chen, D. P. Chang, J. M. Zhang, R. Jordan, S. Zauscher, *Adv. Funct. Mater.* **2012**, *22*, 429.
[19] G. L. Whiting, H. J. Snaith, S. Khodabakhsh, J. W. Andreasen, D. Breiby, M. M. Nielsen, N. C. Greenham, P. H. Friend, W. T. S. Huck, *Nano Lett.* **2006**, *6*, 573.
[20] J. C. Pinto, G. L. Whiting, S. Khodabakhsh, L. Torre, A. B. Rodriguez, R. M. Dalgliesh, A. M. Higgins, J. W. Andreasen, M. M. Nielsen, M. Geoghegan, W. T. S. Huck, H. Sirringhaus, *Adv. Funct. Mater.* **2008**, *18*, 36.
[21] X. Wang, H. Hu, Y. Shen, X. Zhou, Z. Zheng, *Adv. Mater.* **2011**, *23*, 3090.
[22] F. Zhou, W. T. S. Huck, *Phys. Chem. Chem. Phys.* **2006**, *8*, 3815.
[23] A. Hucknall, S. Rangarajan, A. Chilkoti, *Adv. Mater.* **2009**, *21*, 2441.
[24] W. Hu, Y. Liu, Z. Lu, C. M. Li, *Adv. Funct. Mater.* **2010**, *20*, 3497.
[25] E. M. Benetti, C. Acikgoz, X. Sui, B. Vratzov, M. A. Hempenius, J. Huskens, G. J. Vancso, *Adv. Funct. Mater.* **2011**, *21*, 2088.

[26] I. Luzinov, S. Minko, V. V. Tsukruk, *Soft Matter* **2008**, *4*, 714.
[27] X. Q. Liu, X. C. Zhou, Y. Li, Z. J. Zheng, *Chem.-Asian J.* **2012**, *7*, 862.
[28] M. P. Stoykovich, M. Muller, S. O. Kim, H. H. Solak, E. W. Edwards, J. J. de Pablo, P. F. Nealey, *Science* **2005**, *308*, 1442.
[29] H. O. Jacobs, G. M. Whitesides, *Science* **2001**, *291*, 1763.
[30] P. Mesquida, A. Stemmer, *Adv. Mater.* **2001**, *13*, 1395.
[31] H. Fudouzi, M. Kobayashi, N. Shinya, *Adv. Mater.* **2002**, *14*, 1649.
[32] C. R. Barry, J. Gu, H. O. Jacobs, *Nano Lett.* **2005**, *5*, 2078.
[33] S. D. Tzeng, K. J. Lin, J. C. Hu, L. J. Chen, S. Gwo, *Adv. Mater.* **2006**, *18*, 1147.
[34] E. Palleau, N. M. Sangeetha, G. Viau, J. D. Marty, L. Ressier, *ACS Nano* **2011**, *5*, 4228.
[35] D. Zhao, L. T. Duan, M. Q. Xue, W. Ni, T. B. Cao, *Angew. Chem. Int. Ed.* **2009**, *48*, 6699.
[36] G. Lee, Y. H. Shin, J. Y. Son, *J. Am. Chem. Soc.* **2009**, *131*, 1634.
[37] D. Zhao, A. D. Martinez, X. L. Xi, X. L. Ma, N. Wu, T. B. Cao, *Small* **2011**, *7*, 2326.
[38] X. L. Xi, D. Zhao, F. Tong, T. B. Cao, *Soft Matter* **2012**, *8*, 298.
[39] L. Seemann, A. Stemmer, N. Naujoks, *Nano Lett.* **2007**, *7*, 3007.
[40] C. Liu, A. J. Bard, *Nat. Mater.* **2008**, *7*, 505.
[41] C. Liu, A. J. Bard, *J. Am. Chem. Soc.* **2009**, *131*, 6397.
[42] X. L. Ma, D. Zhao, M. Q. Xue, H. Wang, T. B. Cao, *Angew. Chem. Int. Ed.* **2010**, *49*, 5537.
[43] J. U. Park, S. Lee, S. Unarunotai, Y. G. Sun, S. Dunham, T. Song, P. M. Ferreira, A. G. Alleyene, U. Paik, J. A. Rogers, *Nano Lett.* **2010**, *10*, 584.
[44] J. J. Cole, C. R. Barry, X. Y. Wang, H. O. Jacobs, *ACS Nano* **2010**, *4*, 7492.
[45] *Electrets*, 3rd ed. (Ed: G. M. Sessler), Laplacian, Morgan Hill, **1998**.
[46] D. M. Jones, A. A. Brown, W. T. S. Huck, *Langmuir* **2002**, *18*, 1265.
[47] P. Mesquida, *PhD thesis, ETH Zürich* **2002**.
[48] L. Ressier, V. Le Nader, *Nanotechnology* **2008**, *19*.
[49] E. Palleau, L. Ressier, L. Borowik, T. Melin, *Nanotechnology* **2010**, *21*.
[50] X. Zhou, W. L. Xu, Y. Wang, Q. Kuang, Y. F. Shi, L. B. Zhong, Q. Q. Zhang, *J. Phys. Chem. C* **2010**, *114*, 19607.